Time-resolved photoluminescence characterization of oxygen-related defect centers in AlN

Genji, Kumihiro

Uchino, Takashi

(Citation)
Applied Physics Letters,109(2):021113-021113

(Issue Date)
2016-07-11

(Resource Type)
journal article

(Version)
Version of Record

Time-resolved photoluminescence characterization of oxygen-related defect centers in AlN

Kumihiro Genji and Takashi Uchino

Citation: Appl. Phys. Lett. **109**, 021113 (2016); doi: 10.1063/1.4958891
View online: http://dx.doi.org/10.1063/1.4958891
View Table of Contents: http://aip.scitation.org/toc/apl/109/2
Published by the American Institute of Physics

Time-resolved photoluminescence characterization of oxygen-related defect centers in AlN

Kumihiro Genji and Takashi Uchino[a)]
Department of Chemistry, Graduate School of Science, Kobe University, Nada, Kobe 657-8501, Japan

(Received 13 May 2016; accepted 3 July 2016; published online 14 July 2016)

Time-resolved photoluminescence (PL) spectroscopy has been employed to investigate the emission characteristics of oxygen-related defects in AlN in the temperature region from 77 to 500 K. Two PL components with different decay constants are observed in the near-ultraviolet to visible regions. One is the PL component with decay time of <10 ns and its peak position shifts to longer wavelengths from ~350 to ~500 nm with increasing temperature up to 500 K. This PL component is attributed to the radiative relaxation of photoexcited electrons from the band-edge states to the ground state of the oxygen-related emission centers. In the time region from tens to hundreds of nanoseconds, the second PL component emerges in the wavelength region from 300 to 400 nm. The spectral shape and the decay profiles are hardly dependent on temperature. This temperature-independent PL component most likely results from the transfer of photoexcited electrons from the band-edge states to the localized excited state of the oxygen-related emission centers. These results provide a detailed insight into the radiative relaxation processes of the oxygen-related defect centers in AlN immediately after the photoexcitation process. *Published by AIP Publishing*.
[http://dx.doi.org/10.1063/1.4958891]

Aluminum nitride (AlN) is a direct band gap semiconductor with a band gap of ~6 eV at room temperature.[1] Because of its wide band gap nature, AlN is one of the promising materials for optical application in the deep ultraviolet (UV) spectral range. Recently, an AlN-based light-emitting diode with a wavelength of 210 nm has been realized by controlling p-type and n-type doping in AlN thin films[2] and Al(Ga)N nanowires.[3] It should be noted, however, that synthesis of high quality AlN samples is still quite challenging, often resulting in defect-induced transitions in the sub-band gap region[4,5] and the related yellow coloration.[6] Since AlN exhibits a large affinity for oxygen as an impurity, oxygen-related defect centers, such as substitutional O (O_N) defects, are commonly observed impurities in AlN.[7–11] Note also that the substitution of oxygen on nitrogen sites is accompanied by the formation of aluminum vacancies (V_{Al}) for charge compensation.[7,9,10,12] Accordingly, various types of native defects and their complexes are expected to exist in AlN,[13,14] showing a variety of absorptions and emissions in the near UV (NUV) and visible spectral regions.[9,10,15–18]

Among other deep level emissions, a NUV luminescence band centered at ~380 nm (~3.3 eV) is the most frequently observed emission in AlN.[9,10,15,19–25] The NVU emission in AlN can be observed by a variety of luminescence measurements, including photoluminescence (PL),[9,10,15,17,19–24] cathodoluminescence (CL),[25–27] thermoluminescence (TL),[28] and optically stimulated luminescence (OSL).[28] A defect complex comprising V_{Al} and O_N, such as $(V_{Al}-O_N)^-$ or $(V_{Al}-O_N)^{2-}$, is most likely to be responsible for the NUV emission.[10,15–17,21–24] It has also been well established that the NUV emission exhibits a slow decay (or "afterglow") with time constants ranging from milliseconds to hundreds of seconds,[10,21,29] accompanied by a large shift in the energy of the emission peak toward lower energies with increasing delay time.[10,21] These emission features suggest that carrier trapping and the subsequent slow release of trapped carriers play a vital role in the radiative recombination processes of the relevant oxygen-related defect centers in AlN.

Although the slow decay dynamics of the NUV band in AlN has been well recognized and analyzed in the past decades,[10,21] the decay dynamics of the NUV emission just after excitation, or in the time range of nanoseconds, has not been investigated. It should be noted, however, that the information on such fast decay dynamics is of relevance and value for full understanding of the mechanism of the defect related emission in AlN. Therefore, in this work, we perform a detailed time-resolved PL investigation of the NUV emission in AlN powders using the fourth harmonic (266 nm) of a nanosecond Nd:YAG laser pulse as an excitation source. We have found that a very broad PL band in the wavelength region from ~300 to ~700 nm emerges within a few nanoseconds after excitation. The emission maximum of this broad PL band shows a substantial red shift with increasing temperature. On a timescale of tens of nanoseconds after excitation, an additional PL band emerges on the higher energy side of the initial PL band. The decay profile as well as the peak wavelength of this PL band is virtually temperature independent, suggesting a highly localized nature of the emission level. On the basis of these experimental results, we present a possible model for the optical excitation and relaxation processes of the oxygen-related defect centers in AlN immediately after photoexcitation.

We used a commercial AlN powder (Kojundo Kagaku Co., 99.9% in purity) as a raw material. Since the intensity of the NUV PL band for the as-received AlN powder was rather low, as will be shown below, we first heated the AlN

[a)]Author to whom correspondence should be addressed. Email: uchino@kobe-u.ac.jp

powder under flowing N_2 environment in a graphite crucible by using a high-frequency induction heating unit, which is rated at 4 kW at a maximum frequency of 420 kHz. The heating temperature was raised up to ~1900 °C at a rate of ~500 °C/min and maintained at the same temperature for 3 min. The N_2-treated AlN sample was then annealed at 1000 °C for 1 h in an air atmosphere to induce oxygen-related defect centers. We should note that the high-temperature N_2 treatment is effective to suppress the growth of the α-Al_2O_3 phase during the post air annealing process, as shown in the X-ray diffraction (XRD) pattern given in Fig. 1(a). Indeed, when the AlN sample is directly annealed at 1000 °C in air, diffraction peaks ascribed to α-Al_2O_3 were detected in the XRD pattern (not shown here). We then measured steady state PL spectra with a spectrofluorometer (JASCO, FP6600) by exciting with a monochromated Xe lamp (150 W). As shown in Fig. 1(b), the intensity of the NUV PL and PL excitation (PLE) spectra for the N_2/air treated sample is more than ten times larger than that for the as-received sample. This indicates that the present N_2/air treatment is effective to obtain the AlN powder with high NUV PL intensity. In this work, we hence use the N_2/air treated sample to investigate the NUV PL properties of the oxygen-related defect centers in AlN.

We first explore the temperature dependence of the steady state PL properties of the N_2/air treated AlN sample. Figure 2 shows the PL and PLE spectra observed in the temperature range from 77 to 500 K by using a closed cycle N_2 cryostat. One sees from Fig. 2(a) that the peak wavelength of the PL spectra (~370 nm) is almost constant irrespective of temperature. Such a temperature insensitive nature of the NUV PL peak has also been reported previously.[10,25] It should be noted, however, that the peak maximum of the PLE spectra (~250 nm) shows a substantial red shift with increasing temperature (see Fig. 2(b)). As shown in the inset of Fig. 2(b), the temperature dependence of the PLE peak maximum can be well described by the following Bose–Einstein expression,[30] which is often used to describe the temperature dependence of the band gap of various semiconductors, including Ge,[30] GaAs,[31] GaN,[32] and AlN[32,33]

$$E(T) = a - b\left(1 + \frac{2}{\exp\left(\frac{\hbar\omega}{k_B T}\right) - 1}\right), \qquad (1)$$

where the parameters a, b, and θ represent the band-gap energy at 0 K, the strength of the electron–phonon coupling, and the average phonon energy, respectively. The fitted values reported previously for AlN single crystals are $b = 471$

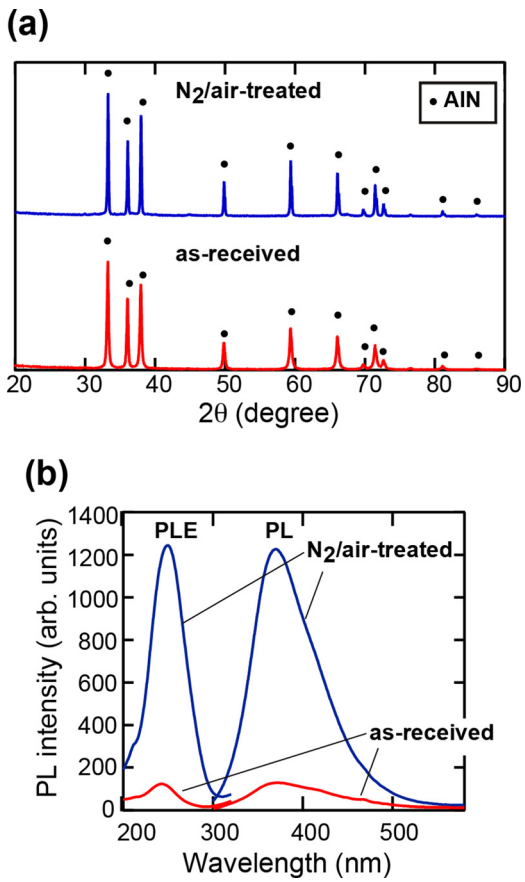

FIG. 1. (a) X-ray diffraction patterns and (b) PL and PLE spectra of the as-received and N_2/air treated AlN samples. These measurements were carried out at room temperature.

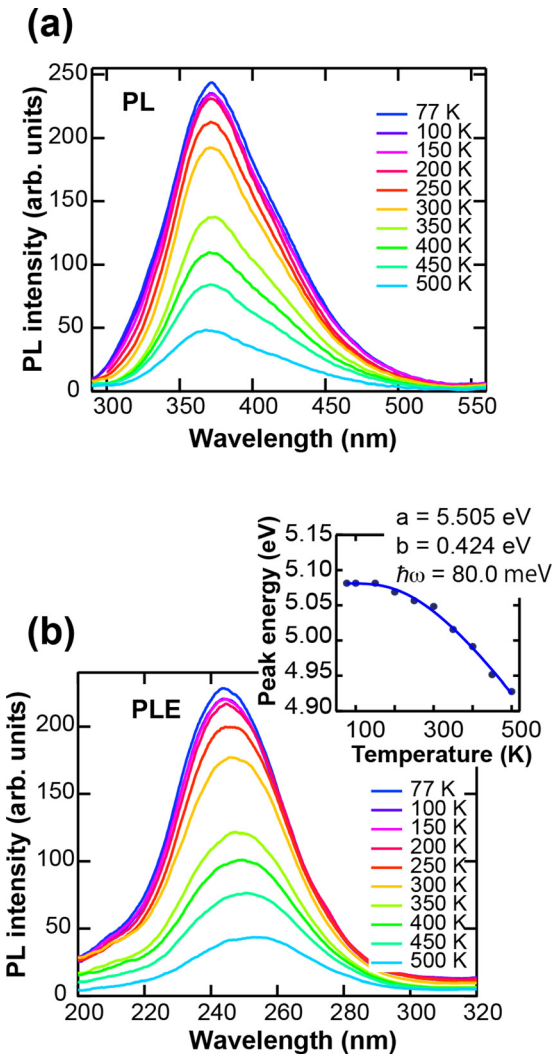

FIG. 2. (a) PL and (b) PLE spectra of the N_2/air treated AlN sample measured in the temperature range of 77–500 K. The inset in (b) shows the temperature dependence of the peak energy of the PLE spectra. The solid curve is the fit of Eq. (1).

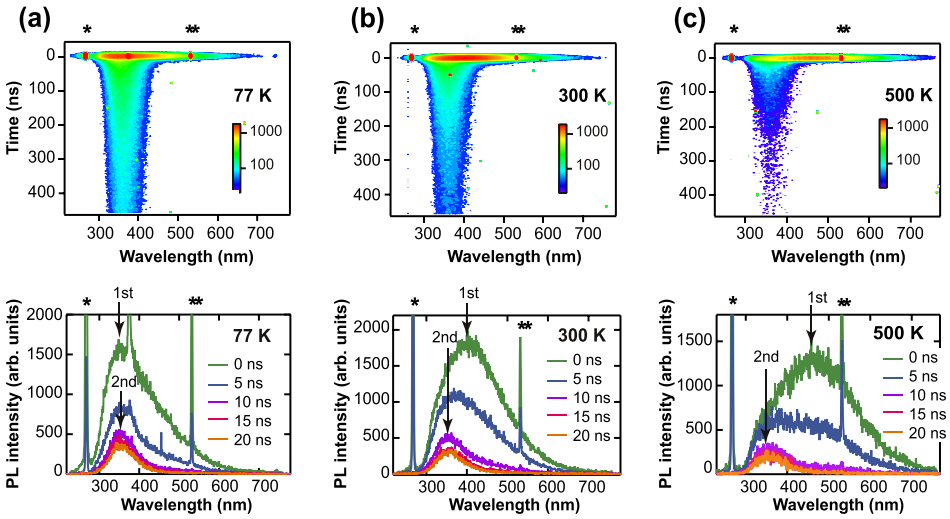

FIG. 3. Time-resolved PL spectra of the N_2/air treated AlN sample measured at (a) 77, (b) 300, and (c) 500 K under excitation with a frequency-quadrupled pulsed Nd:YAG laser (266 nm). The upper and lower panels show, respectively, the false color contour plots of the PL spectra in the 0–460 ns time range and the corresponding typical time-resolved PL spectra after delay times of 0–20 ns. The single and double asterisks indicate the fourth (266 nm) and contaminated third (355 nm) harmonics of the incident Nd:YAG laser beam, respectively. The peak positions of the first and second PL components are marked by arrows.

-670 meV and $\hbar\omega = 62-86$ meV.[32,33] These reported values are in reasonable agreement with those we obtained here, i.e., $b = 424$ meV and $\hbar\omega = 80$ meV. It should also be noted that in AlN, the average phonon energy is estimated to be 81 meV,[34] which agrees well with the value obtained in this work ($\hbar\omega = 80$ meV). Thus, we consider that the temperature dependence of the PLE peak maximum is governed by the electron–phonon interactions, as in the case of the temperature dependent band-gap shift. This allows us to suggest that as for the NUV emission in AlN, the temperature-sensitive photoabsorption process is not a simple reverse of the radiative transition process, which is basically temperature insensitive in terms of emission wavelength.

To obtain further insight into the photoabsorption and the resulting emission processes, we carried out time-resolved PL measurements using the fourth harmonic (266 nm) of a nanosecond Nd:YAG laser pulse as an excitation source. Figure 3 shows false color contour plots of the time-resolved PL intensity measured at different temperatures of 77, 300, and 500 K, along with the corresponding typical time-resolved PL spectra after delay times of 0–20 ns from excitation. One sees from Fig. 3 that there exist two PL components with different decay constants on the time scale of nanoseconds. One is the PL component whose decay time constant is <10 ns. The spectral width of this PL component is quite broad, ranging from 300 to 700 nm. Note also that the peak maximum of this PL component, whose maximum is defined as the peak position of the time-resolved spectra observed at the delay time of 0 s, shows a red shift with increasing temperature, as also shown in Fig. 4(a). In Fig. 3(a), one also notices a sharp peak at $\sim$380 nm in the time-resolved PL spectrum recorded at a delay time of 0 s. We found that such a sharp peak at $\sim$380 nm is observed commonly in the low temperature region below $\sim$100 K. This peak does not result from the incident laser light but could be attributed to a light amplification process occurring only at low temperatures during photoexcitation. At present, however, its physical origin is unclear, and further work needs to be done for a better understanding of this sharp peak feature. Figure 3 further reveals that the second PL component emerges on a timescale of tens of nanoseconds after excitation. The peak maximum of the second PL component can

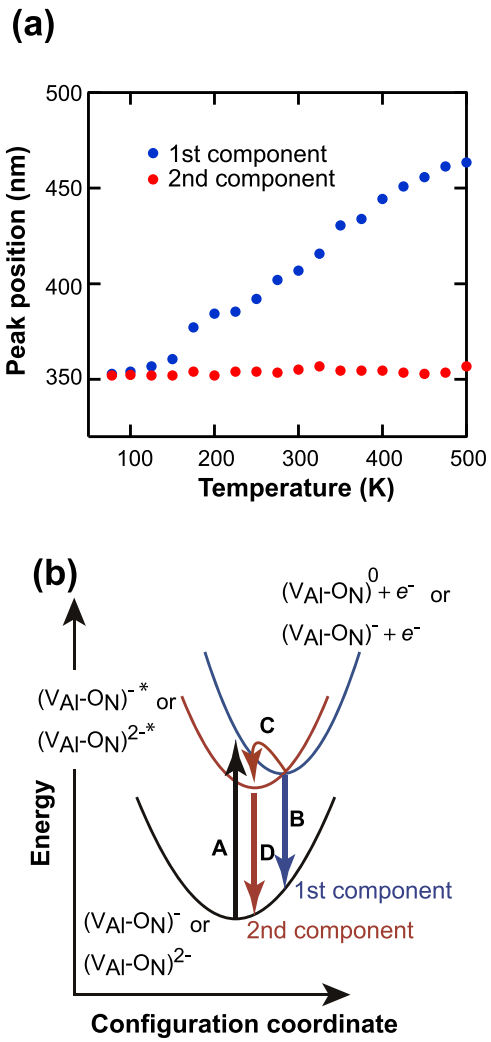

FIG. 4. (a) Temperature dependence of the peak position of the first and second PL components observed in the time-resolved PL measurements shown in Fig. 3. (b) Configuration coordinate diagram for the transition between an electron in a deep accepter state ($(V_{Al}\text{-}O_N)^-$ or $(V_{Al}\text{-}O_N)^{2-}$) and the band-edge state ($(V_{Al}\text{-}O_N)^0 + e^-$ or $(V_{Al}\text{-}O_N)^- + e^-$) (process A) and the subsequent first (process B) and second (process D) emission processes. Process C indicates the electron transfer from the band edge state to the excited state of a deep acceptor state.

be defined as the peak position of the time-resolved spectra observed at the delay time of >15 ns.

As shown in Fig. 5, the decay curves of the present NUV PL emission, including both the first and second PL components, can be fitted with a triple exponential function

$$I(t) = I_1 \exp\left(-\frac{t}{\tau_1}\right) + I_2 \exp\left(-\frac{t}{\tau_2}\right) + I_3 \exp\left(-\frac{t}{\tau_3}\right), \quad (2)$$

where $I(t)$ is the PL intensity at time t and I_i and τ_i represent, respectively, the initial intensity and the decay time constant of the i-th component. It has also been found that all the fitted decay time constants are temperature insensitive, yielding the values of $\tau_1 \sim 5$, $\tau_2 \sim 50$, and $\tau_3 \sim 400$ ns. The fast decay constant (τ_1) will represent the effective radiative lifetime of the first PL component, whereas the other decay constants (τ_2 and τ_3) will characterize the decay dynamics of the second PL component. Thus, the observed triple exponential decay profile is considered to result from the combination of the first PL component with a single exponential decay ($\tau_1 \sim 5$ ns) and the second PL component with a double exponential decay ($\tau_2 \sim 50$ ns and $\tau_3 \sim 400$ ns).

From the present time-resolved PL measurements, we propose a scheme for the NUV emission process just after photoexcitation as follows. Since the temperature dependence of the PLE peak energy is well described by Eq. (1), as in the case of semiconductor band gaps, optical transition to (or from) band-edge states will be responsible for the first excitation process. The absorption features in the 3.5–5 eV (350–250 nm) range are commonly attributed to $(V_{Al}\text{-}O_N)$ type complexes.[9,10,16,18] Thus, we consider that the photoexcitation process related to the NUV PL most likely results from the ionizing transition from such a complex in the form of $(V_{Al}\text{-}O_N)^-$ or $(V_{Al}\text{-}O_N)^{2-}$ to the conduction band-edge states (process A in Fig. 4(b)). Furthermore, the present time-resolved PL measurements have revealed two types of emissions with different decay constants on the time scale of nanoseconds. We consider that the first emission process with a decay time constant of $\tau_1 \sim 5$ ns is attributed to the reverse of the photoabsorption, i.e., radiative relaxation from the conduction band-edge states to $(V_{Al}\text{-}O_N)^-$ or $(V_{Al}\text{-}O_N)^{2-}$ (process B in Fig. 4(b)). The highly temperature-sensitive nature of the peak wavelength of this emission is also consistent with our assumption that the band-edge states are involved in the first emission process. On the other hand, the decay profile of the second emission process, which is characterized by a double exponential function with $\tau_2 \sim 50$ ns and $\tau_3 \sim 400$ ns, is temperature insensitive and is too long to be accounted for any direct radiation process. The emission peak wavelength of the second emission is also temperature independent, suggesting the highly localized nature of the emission state. Such a temperature-insensitive double exponential decay in the time scale of nanoseconds has been previously reported for defect-related localized emissions in Si-doped GaAs[35] and silica-based nanostructured materials.[36] As for these defect-related emissions, the electron in the localized emission state will not compete with any of the existing nonradiative processes, leading to the temperature-insensitive decay dynamics.[35,36] We consider that the above emission scheme can also be applied to the second emission process observed in AlN. That is, the second emission process will result from the transfer of photoexcited electrons from the band-edge state to the localized excited state of the $(V_{Al}\text{-}O_N)^-$ or $(V_{Al}\text{-}O_N)^{2-}$ complex (process C in Fig. 4(b)), resulting in the radiative recombination with temperature insensitive decay constants of several tens of nanoseconds (process D in Fig. 4(b)). The observed two decay time constants of $\tau_2 \sim 50$ and $\tau_3 \sim 400$ ns suggest the presence of certain trapping and detrapping processes of the charge carriers via shallow traps, which will be located several tens of meV below the conduction band edge, during the electron transfer process, as has often been observed in trap-related emissions in III-V nitride semiconductors.[37,38]

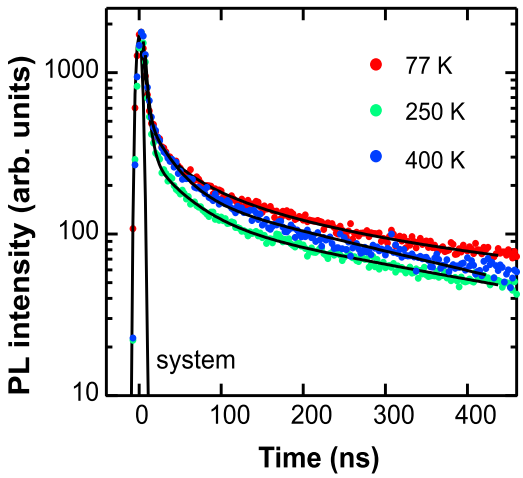

FIG. 5. The PL decay profiles of the emission band in the 300–400 nm region measured at 77, 250, and 400 K. The solid lines show the fit to a triple exponential function (Eq. (2)).

These nanosecond PL decay components have not been reported or been paid attention so far. This is probably because AlN exhibits a striking long-lasting emission extending up to several seconds.[10,19,21,29] It is hence interesting to investigate whether the present N_2/air-treated AlN sample has a long-lasting decay channel or not. For that purpose, we measured the time-resolved PL spectra in the 1 ms–10 s time window by using a monochromated Xe lamp (250 nm) and a mechanical shutter. Similar to the case of the previous results,[10,21] the present sample shows a slow decay on the time scale of seconds or longer (Fig. S1(a) in supplementary material[39]), and a red shift of the luminescence peak with delay time is also observed (Fig. S1(b)[39]). Thus, we consider that in AlN the long-lasting PL is possible to coexist with the nanosecond PL decay components. The long-lasting PL will occur when the photoexcited electrons are transferred indirectly from the band-edge state to the emission level via long-lived or deep charge traps.[21,29,40,41] On the other hand, immediate transfer of the photoexcited electrons to the emission level (occasionally via short-lived or shallow charge traps) will be responsible for the radiative emission process on the time scale of several tens of nanoseconds, as observed in the form of the second PL component in this work.

In summary, we have shown from the time-resolved and temperature dependent PL measurements that the defect-related emission in AlN exhibits complicated decay dynamics on the time scale of nanoseconds. A very broad PL emission

with decay time of <10 ns is observed in the wavelength region from 300 to 700 nm just after photoexcitation. The peak wavelength of the first PL decay component shows a substantial red shift with increasing temperature. A second PL component emerges on the higher-energy side of the initial PL band within tens of nanoseconds after excitation. The decay profile of this PL component is well represented by a triple exponential function with temperature-insensitive time constants of $\sim$5, $\sim$50, and $\sim$400 ns. Note also that the peak wavelength of this slow PL component is also temperature insensitive. From the results of the above time-resolved PL measurements, we propose that the initial PL component results from the reverse of the photoabsorption process, i.e., the radiative transition from the conduction band-edge states to the ground sate of the $(V_{Al}\text{-}O_N)^{n-}$ defect complex, whereas the transfer of photoexcited electrons from the band-edge state to the excited (emission) state of $(V_{Al}\text{-}O_N)^{n-}$ defect complex is responsible for the second PL component. These nanosecond PL decay characteristics will not only shed light on the emission mechanism of the oxygen-defect related emission in AlN immediately after the photoexcitation event, but will also give a further insight into the mechanism of the PL component in the NUV region.

[1]W. M. Yim, E. J. Stofko, P. J. Zanzucchi, J. I. Pankove, M. Ettenberg, and S. L. Gilbert, J. Appl. Phys. **44**, 292 (1973).
[2]Y. Taniyasu, M. Kasu, and T. Makimoto, Nature **441**, 325 (2006).
[3]S. Zhao, A. T. Connie, M. H. T. Dastjerdi, X. H. Kong, Q. Wang, M. Djavid, S. Sadaf, X. D. Liu, I. Shih, H. Guo, and Z. Mi, Sci. Rep. **5**, 8332 (2015).
[4]P. B. Perry and R. F. Rutz, Appl. Phys. Lett. **33**, 319 (1978).
[5]V. V. Michailin, V. E. Oranovskii, S. Pačesová, J. Pastrňák, and A. S. Salamatov, Phys. Status Solidi B **55**, K51 (1973).
[6]A. Sedhain, L. Du, J. H. Edgar, J. Y. Lin, and H. X. Jiang, Appl. Phys. Lett. **95**, 262104 (2009).
[7]G. A. Slack, J. Phys. Chem. Solids **34**, 321 (1973).
[8]M. Benabdesselam, P. Iacconi, D. Lapraz, P. Grosseau, and B. Guilhot, J. Phys. Chem. **99**, 10319 (1995).
[9]J. Pastrňák, S. Pačesová, and L. Roskovocová, Czech. J. Phys. B **24**, 1149 (1974).
[10]R. A. Youngman and J. H. Harris, J. Am. Ceram. Soc. **73**, 3238 (1990).
[11]M. Bickermann, B. M. Epelbaum, and A. Winnacker, J. Cryst. Growth **269**, 432 (2004).
[12]S. M. Evans, N. C. Giles, L. E. Halliburton, G. A. Slack, S. B. Schujman, and L. J. Schowalter, Appl. Phys. Lett. **88**, 062112 (2006).
[13]T. Mattila and R. M. Nieminen, Phys. Rev. B **55**, 9571 (1997).
[14]J.-M. Mäki, I. Makkonen, F. Tuomisto, A. Karjalainen, S. Suihkonen, J. Räisänen, T. Yu. Chemekova, and Yu. N. Makarov, Phys. Rev. B **84**, 081204(R) (2011).
[15]S. Pačesová and L. Jastrabík, Czech. J. Phys. B **29**, 913 (1979).
[16]Q. Yan, A. Janotti, M. Scheffler, and C. B. Van de Walle, Appl. Phys. Lett. **105**, 111104 (2014).
[17]K. B. Nam, M. L. Nakarmi, J. Y. Lin, and H. X. Jiang, Appl. Phys. Lett. **86**, 222108 (2005).
[18]M. Bickermann, A. Münch, B. M. Epelbaum, O. Filip, P. Heimann, S. Nagata, and A. Winnacker, J. Appl. Phys. **103**, 073522 (2008).
[19]F. Karel and J. Pastrňák, Czech J. Phys. B **20**, 46 (1970).
[20]M. Strassburg, J. Senawiratne, N. Dietz, U. Haboeck, A. Hoffmann, V. Noveski, R. Dalmau, R. Schlesser, and Z. Sitar, J. Appl. Phys. **96**, 5870 (2004).
[21]L. Trinkler and B. Berzina, Phys. Status Solidi B **251**, 542 (2014).
[22]X. H. Ji, Q. Y. Zhang, S. P. Lau, H. X. Jiang, and J. Y. Lin, Appl. Phys. Lett. **94**, 173106 (2009).
[23]S.-C. Shi, C. F. Chen, S. Chattopadhyay, K.-H. Chen, B.-W. Ke, L.-C. Chen, L. Trinkler, and B. Berzina, Appl. Phys. Lett. **89**, 163127 (2006).
[24]T. Koyama, M. Sugawara, T. Hoshi, A. Uedono, J. F. Kaeding, R. Sharma, S. Nakamura, and S. F. Chichibu, Appl. Phys. Lett. **90**, 241914 (2007).
[25]T. Schulz, M. Albrecht, K. Irmscher, C. Hartmann, J. Wollweber, and R. Fornari, Phys. Status Solidi B **248**, 1513 (2011).
[26]M. Bickermann, B. Epelbaum, O. Filip, P. Heimann, S. Nagata, and A. Winnacker, Phys. Status Solidi B **246**, 1181 (2009).
[27]B. Bastek, F. Bertram, J. Christen, T. Hempel, A. Dadgar, and A. Krost, Appl. Phys. Lett. **95**, 032106 (2009).
[28]L. Trinkler, L. Bøtter-Jensen, P. Christensen, and B. Berzina, Radiat. Meas. **33**, 731 (2001).
[29]A. S. Vokhmintsev, I. A. Weinstein, and D. M. Spiridonov, J. Lumin. **132**, 2109 (2012).
[30]L. Viña, S. Logothetidis, and M. Cardona, Phys. Rev. B **30**, 1979 (1984).
[31]P. Lautenschlager, M. Garriga, S. Logothetidis, and M. Cardona, Phys. Rev. B **35**, 9174 (1987).
[32]K. B. Nam, J. Li, j. Y. Lin, and H. X. Jiang, Appl. Phys. Lett. **85**, 3489 (2004).
[33]Q. Guo, M. Nishio, H. Ogawa, and A. Yoshida, Phys. Rev. B **64**, 113105 (2001).
[34]*Gallium Nitride and Related Semiconductors*, edited by J. H. Edgar, S. Strite, I. Akasaki, H. Amano, and C. Wetzel (Inspec, London, 1999).
[35]T. Sauncy, C. P. Palsule, M. Holtz, and S. Gangopadhyay, Phys. Rev. B **53**, 1900 (1996).
[36]N. Sagawa and T. Uchino, Appl. Phys. Lett. **87**, 251923 (2005).
[37]M. S. Minsky, S. Watanabe, and N. Yamada, J. Appl. Phys. **91**, 5176 (2002).
[38]T. Onuma, S. F. Chichibu, A. Uedono, T. Sota, P. Cantu, T. M. Katona, J. F. Keading, S. Keller, U. K. Mishra, S. Nakamura, and S. P. DenBaars, J. Appl. Phys. **95**, 2495 (2004).
[39]See supplementary material at http://dx.doi.org/10.1063/1.4958891 for the results of time-resolved PL measurements in the time range after 1 ms.
[40]I. A. Weinstein, A. S. Vokhmintsev, and D. M. Spiridonov, Diamond Relat. Mater. **25**, 59 (2012).
[41]L. Jin, H. Zhang, R. Pan, Pi. Xu, J. Han, X. Zhang, Q. Yuan, Z. Zhang, X. Wang, Y. Wang, and B. Song, Nano Lett. **15**, 6575 (2015).